Investigation of Gamma Radiation Shielding Properties of High-Z-Doped Multilayer PVA Polymers

G.B. Hiremath[a], V.P. Singh[b], N.H. Ayachit[a] and N.M. Badiger[a,*]

[a] *School of Advanced Sciences, KLE Technological University, Hubbali-580031, India*
[b] *Department of Physics, Karnatak University, Dharwad-580008, India*

Received: 16.07.2024 & Accepted: 03.09.2024

Doi: 10.12693/APhysPolA.146.285 *e-mail: nbadiger@gmail.com

Multilayer polymers have potential applications in various fields for radiation shielding. It is quite interesting to investigate the shielding properties of polymer composites in a combined manner. In the present investigations, the high-Z-doped PVA polymers such as PVA+50%Bi_2O_3 and PVA+50%Na_2O_4W were selected, and the multilayer buildup factors were calculated for various combinations of high-Z-doped multilayer PVA polymers using the Py-MLBUF software. The PVA+50%Bi_2O_3 and PVA+50%Na_2O_4W are coded, respectively, as A and B. The BA and BBA combinations have the potential to replace a single layer of high-Z-doped PVA polymers, and these combinations can be used as gamma-ray shields.

topics: radiation shielding, polymers, multilayer shields, buildup factor

1. Introduction

Ionizing radiation is used in various areas such as medical imaging, cancer treatment, food preservation, power generation, and trace elemental analysis. These radiations can also interact with living things by damaging tissues and DNA in genes. Therefore, appropriate radiation shielding materials are in demand for secure life and healthy environment. Materials such as polymers, alloys, concrete, bricks, and glasses are used in radiation shielding applications. Although lead and concrete are appropriate materials for shielding ionizing radiation in various fields, these two have several drawbacks, i.e., lead is hazardous to human health and environment, and the variation of moisture in concrete makes it difficult to predict radiation protection [1].

It has been found recently that gamma radiation is shielded by the addition of high-Z material to polymers. In this direction, several researchers have studied high-Z-doped polymers for radiation shielding applications [2, 3]. The limitation of void paths that are present in a single layer can be reduced in multilayer radiation shielding materials. Several layers of materials, each layer having a uniform distribution of doped materials, would create densely packed structures without leaving pinholes in the composites. This is how multilayer radiation shielding materials overcome this by reducing the void paths for photons to penetrate and enhancing radiation attenuation probability. Several researchers have studied multilayer radiation shielding materials as radiation shields [4–8].

From the literature survey, it has been concluded that high-Z-doped polymers act as radiation shields, and multilayer radiation shields overcome void paths. However, it is interesting to understand which combination of polymer composites has the most potential to shield gamma radiation. To the best knowledge of the authors, no study was carried out to understand which combination of multilayer radiation shields acts as the best radiation shield. In the present investigations, high-Z-doped PVA polymers such as PVA+50%Bi_2O_3 and PVA+50%Na_2O_4W were selected [9, 10]. Double layer and triple layer gamma ray buildup factors for different combinations were calculated using the Py-MLBUF [11] software. Mass attenuation coefficient (MAC), half value layer (HVL), tenth value layer (TVL), and effective atomic number (Z_{eff}) were estimated for a single layer of PVA+50%Bi_2O_3 and PVA+50%Na_2O_4W using the Py-MLBUF software as well. The MAC values were compared with the values from the XCOM database in order to validate our calculated results.

2. Materials and methods

The high-Z-doped polymers, such as PVA+50% Bi_2O_3 and PVA+50%Na_2O_4W, were selected in the present investigations [9, 10], and the densities of these selected polymers are shown in Table I. The combinations of double and triple layers of selected high-Z-doped PVA polymers are shown in Fig. 1. It has been observed that there are only two combinations, namely AB, BA, for double layer and six combinations, namely AAB, ABA, ABB, BAA, BAB, and BBA, for triple layer of high-Z-doped PVA polymers.

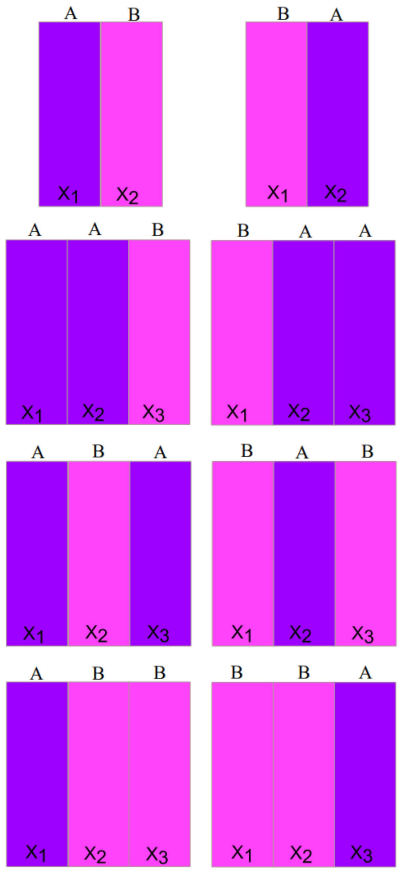

Fig. 1. The combinations of double and triple layers of high-Z-doped PVA polymers. Here, A denotes PVA+50% Bi_2O_3 and B denotes PVA+50% Na_2O_4W; X_1, X_2, and X_3 denote penetration depth (in units of mean free path) of first, second, and third layer, respectively.

TABLE I

The selected high-Z-doped PVA polymers and their density.

Samples	Code	Density [g/cm^3]
PVA+50%Bi_2O_3	A	1.61
PVA+50%Na_2O_4W	B	1.543

Parameters: MAC, HVL, TVL, and Z_{eff} were calculated for a single layer of PVA+50%Bi_2O_3 and PVA+50%Na_2O_4W, as explained elsewhere [12–20]. In the present investigations, double layer and triple layer gamma ray buildup factors were estimated for selected polymers using the Py-MLBUF [11] software.

2.1. Buildup factor for single-layered shields

The buildup factors are correction factors, which accounts for the influence of scattered radiation and secondary particles in the materials. EBF and EABF represent buildup factors for single-layered shields. The computational work for EBF and EABF was done in three steps, as given below [12, 21]:

(i) Calculation of the equivalent atomic number (Z_{eq});

(ii) Calculation of the geometrical progression (GP) fitting parameters;

(iii) Calculation of the exposure and energy absorption buildup factors.

The equivalent atomic number Z_{eq} compares the characteristics of composite materials made of equivalent elements to the characteristic of a single element's atomic number. The gamma photon interactions with matter are generally known to occur through photoelectric absorption, Compton scattering, and pair creation. The Compton scattering interaction process forms Z_{eq}. However, the buildup factor of photons in the material is mainly caused by several Compton scattering events. Thus, Z_{eq} can be expressed as the Compton mass attenuation coefficient ratio relative to the total mass attenuation coefficient at the specific photon energy,

$$Z_{eq}=\frac{Z_1\big[\log(R_2)-\log(R)\big]+Z_2\big[\log(R)-\log(R_1)\big]}{\log(R_2)-\log(R_1)}, \tag{1}$$

where Z_1 and Z_2 are the atomic numbers of the elements corresponding to the ratios R_1 and R_2, respectively. The ratio R is equal to $(\frac{\mu}{\rho})_{\text{compton}}/(\frac{\mu}{\rho})_{\text{total}}$ for chosen samples at the specific energy [13].

The estimation of Z_{eq} is achieved by the interpolation method. Likewise, the parameters for GP fitting associated with selected samples are estimated using a comparable formula, described as

$$P=\frac{P_1\big[\log(Z_2)-\log(Z_{eq})\big]+P_2\big[\log(Z_{eq})-\log(Z_1)\big]}{\log(Z_2)-\log(Z_1)}, \tag{2}$$

where P_1 and P_2 are the values of GP fitting parameters (b, c, a, X_k, d) corresponding to the atomic numbers of Z_1 and Z_2, respectively, at the specific energy.

Ultimately, by employing GP fitting parameters (b, c, a, X_k, d) within the energy spectrum of 0.015–15 MeV and up to a penetration depth of 40 mfp, the buildup factors were calculated using specific equations [21]

$$B\,(E,x) = 1 + \frac{b-1}{K-1}\,(K^x - 1) \quad \text{for} \quad K \neq 1, \tag{3}$$

and

$$B\,(E,x) = 1 + (b-1)\,x \quad \text{for} \quad K = 1. \tag{4}$$

The expression $K(E,x)$ denotes the photon dose multiplication factor, which is determined by the equation for $x \leq 40$ mfp

$$K\,(E,x) = c\,x^a + d\frac{\tanh\left(\frac{x}{X_k} - 2\right) - \tanh\,(-2)}{1 - \tanh\,(-2)}, \tag{5}$$

where b is the accumulation factor at 1 mfp, E denotes the energy of the incident photon, and x refers to the distance from the source to the detector within the medium, measured in units of mean free paths (mfp).

2.2. Buildup factors for double-layered shields

The double layer buildup factors (DLEABF and DLEBF) are required for calculating the buildup factors for double-layered shields. And double-layered shields are the simplest case of multilayered shields. M.H. Kalos was the first to propose an empirical formula derived by fitting data based on Monte Carlo simulations for a plain-normal source and double-layered shields composed of lead (3 mfp) + water (3 mfp). He further introduced the orientation concept, which involves the arranging of materials from a high-Z material source followed by low-Z material (HZFLZ), and its opposite configuration, where materials are arranged as follows: a low-Z material followed by high-Z material (LZFHZ). Lin and Jiang [22] (see also [11, 23]) improved the double layer buildup factor by introducing a modification in the correction factor for the point-isotropic source. The equation for estimation of DLEBF and DLEABF is shown below

$$B\,(X_1{,}X_2) = B_2\,(X_2) + K\,(X_1)\,C\,(X_2) \times\Big[B_2\,(X_1{+}X_2) - B_2\,(X_2)\Big], \tag{6}$$

where

$$K\,(X_1) = \frac{B_1\,(X_1) - 1}{B_2\,(X_1) - 1}, \tag{7}$$

$$C\,(X_2) = \begin{cases} \mathrm{e}^{-1.08\beta X_2} + 1.13\beta\; l(-X_2), & \text{HZFLZ}, \\ 0.8\; l(X_2) + \left(\frac{\gamma}{K}\right)\mathrm{e}^{-X_2}, & \text{LZFHZ}. \end{cases} \tag{8}$$

In (6), $B(X_1, X_2)$ refers to DLEBF (or DLEABF) for the double-layered shields with the first layer's penetration depth of X_1 [mfp], followed by the second layer's penetration depth of X_2 [mfp]. The K-parameter (photon dose multiplication factor) for double-layered shields is shown in (7). The function $C(X_2)$ is the modified correction factor for both orientations, as shown in (8).

2.3. Buildup factors for multilayered shields

Further, Lin and Jiang [22] (see also [11, 23]) rewrote the empirical formula to better approximate the buildup factors in multilayered shields made from n-layered media. The generalized empirical formulae used for estimating the n-layered buildup factor are given below [11]

$$B(X_1, X_2, \ldots X_n) = B_n(X_n) + K\,(X_1, X_2, \ldots X_{n-1}) \times C\,(X_n)\left[B_n\Big(\sum_{i=1}^{n} X_i\Big) - B_n(X_n)\right],$$

$$K\,(X_1, X_2, \ldots X_{n-1}) = \frac{B\,(X_1, X_2, \ldots X_{n-1}) - 1}{B_n\left(\sum\limits_{i=1}^{n} X_i\right) - 1}. \tag{10}$$

The equation for the modified corrector factor for the generalized n-layered is given as

$$C\,(X_n) = \begin{cases} \mathrm{e}^{-1.08\beta X_n} + 1.13\beta\; l(-X_n), & \text{HZFLZ}, \\ 0.8\; l(X_n) + \left(\frac{\gamma}{K}\right)\mathrm{e}^{-X_n}, & \text{LZFHZ}, \end{cases} \tag{11}$$

$$\beta = \left(\mathrm{MAC}_{\mathrm{total}}\right)_n / \left(\mathrm{MAC}_{\mathrm{total}}\right)_{n-1}, \tag{12}$$

$$\gamma = \left(\mathrm{MAC}_{\mathrm{compton}}\right)_{n-1} / \left(\mathrm{MAC}_{\mathrm{compton}}\right)_n, \tag{13}$$

$$l\,(X_n) = \frac{B_n(X_{n)} + 1}{B_{n-1}(X_n) + 1}\,\left(1 - \mathrm{e}^{-X_n}\right), \tag{14}$$

where β and γ indicate the ratios of the corresponding gamma shielding parameter for n-th and $(n-1)$-th layers as shown in (12)–(13), respectively. $\mathrm{MAC}_{\mathrm{total}}$ is the total mass attenuation coefficient, and $\mathrm{MAC}_{\mathrm{compton}}$ is the Compton mass attenuation coefficient. In the present investigations, MLEBF and MLEABF were estimated using (9) for $n = 3$.

3. Results and discussion

The MAC values were calculated using the Py-MLBUF software for high-Z-doped PVA polymers such as PVA+50%Bi_2O_3 and PVA+50%Na_2O_4W in the energy range from 0.015 to 15 MeV. The results were compared with the XCOM values in order to validate the calculations. The Python program for multi-layered buildup factor is an acronym of Py-MLBUF, and it is a user-friendly online-platform used by us to calculate gamma ray shielding parameters in the energy range

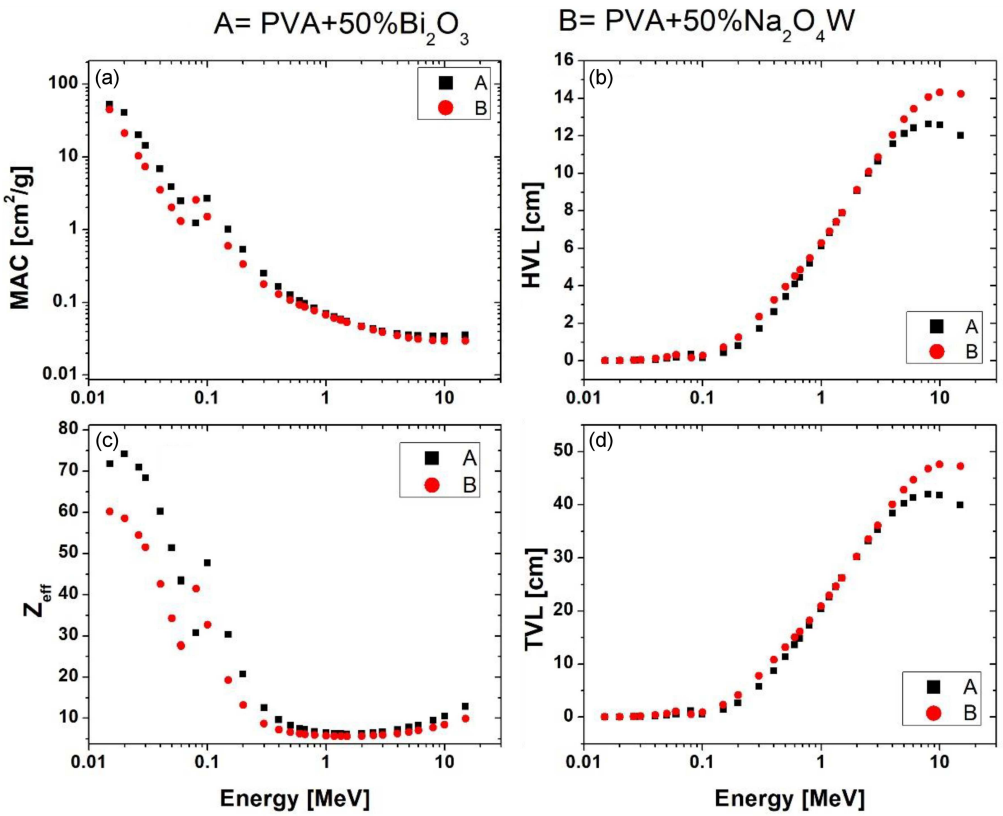

Fig. 2. (a)–(d) Radiation shielding properties of single layer of high-Z-doped PVA polymers such as PVA+50%Bi_2O_3 and PVA+50%Na_2O_4W.

of 0.015–15 MeV. In turn, XCOM is a database of photo cross-sections for elements and compounds and it is maintained by the National Institute of Standards and Technology (NIST) [24]. Table II shows a comparison between the MAC values of high-Z-doped PVA polymers with those from XCOM. Good agreement between the values predicted by Py-MLBUF and XCOM encouraged proceeding calculations of other shielding parameters. Then, HVL, TVL, and Z_{eff} values were calculated for PVA+50%Bi_2O_3 and PVA+50%Na_2O_4W using the Py-MLBUF [11] software, and they are also shown in Fig. 2a–d. The MAC values in the Py-MLBUF software, which are based on the XCOM code, have such minimal uncertainties that they are not shown in the figures due to the high precision of the theoretical calculations based on the XCOM code. It is important to notice from Fig. 2 that the MAC values decrease with increasing energy of gamma photons — except for the K-edge energies of Bi and W. In the lower energy region, the photoelectric absorption process is dominant; in the medium energy region, Compton scattering is dominant; in the higher energy region, the pair production process is dominant. The HVL and TVL values show similar shapes for selected PVA polymers up to 8 MeV. Above 8 MeV, the HVL and TVL values are lower for PVA+50%Bi_2O_3 than PVA+50%Na_2O_4W. The plot of Z_{eff} values versus energy of gamma photons is also shown in Fig. 2c. In the low and high energy region, the Z_{eff} values of PVA+50%Bi_2O_3 are higher than those of PVA+50%Na_2O_4W.

Here, we estimate the double layer exposure buildup factor (DLEBF) and the double layer energy absorption buildup factor (DLEABF) for the selected high-Z-doped polymers. The high-Z polymer PVA+50%Bi_2O_3 is named A, and PVA+50%Na_2O_4W is named B. DLEBF and DLEABF were calculated at selected penetration depths (i.e., $X_1 = 1$ mfp and $X_2 = 1$ mfp) for combinations AB and BA, and they are shown in Fig. 3a–b. Here, X_1 and X_2 indicate the penetration depth [mfp] of the first and second layers, respectively. Figure 3 shows that in the lower energy region around 40 keV, both DLEBF and DLEABF values are higher for BA combination than AB, and in the higher energy region around 1 MeV, the DLEBF values are slightly higher for AB than BA. However, for DLEABF, the values are higher for AB combination than for BA. From this data, it is interesting to note that in the BA combination, the incident gamma photons first interact with the low-Z_{eff} layer and produce a large number of Compton scattered gamma photons. These scattered gamma photons interact with the high-Z_{eff} layer through photoelectric absorption and the pair production processes. It is well known that

TABLE II

MAC values of PVA+50%Bi_2O_3 and PVA+50%Na_2O_4W compared with XCOM values.

Energy [MeV]	MAC [cm^2/g] for PVA+50%Bi_2O_3		MAC [cm^2/g] for PVA+50%Na_2O_4W	
	XCOM	Py-MLBUF	XCOM	Py-MLBUF
0.015	52.670	52.690	44.590	44.593
0.020	40.490	40.483	21.110	21.110
0.026	20.020	19.941	10.340	10.292
0.030	14.310	14.311	7.363	7.363
0.040	6.839	6.838	3.516	3.517
0.050	3.874	3.874	2.012	2.012
0.060	2.505	2.503	1.323	1.322
0.080	1.228	1.228	2.564	2.564
0.100	2.664	2.664	1.500	1.500
0.150	1.015	1.014	0.594	0.593
0.200	0.537	0.537	0.335	0.335
0.500	0.126	0.126	0.107	0.107
0.600	0.105	0.105	0.093	0.093
0.662	0.097	0.097	0.087	0.087
0.800	0.083	0.083	0.077	0.077
1.000	0.070	0.070	0.067	0.067
1.170	0.063	0.063	0.061	0.061
1.330	0.058	0.058	0.057	0.057
1.500	0.055	0.055	0.053	0.053
2.000	0.047	0.047	0.046	0.046
5.000	0.036	0.036	0.033	0.033
6.000	0.035	0.035	0.031	0.031
8.000	0.034	0.034	0.030	0.030
10.000	0.034	0.034	0.029	0.029
15.000	0.036	0.036	0.030	0.030

photoelectric absorption is directly proportional to Z_{eff}^5 and the pair production process is proportional to Z_{eff}^2. This type of similar behavior was observed by Mann et al. (2019) [7].

Figures 4a–d and 5a–d present the plot of DLEBF and DLEABF values versus penetration depth of the second layer (X_2) at incident energies 0.015, 0.15, 1.5, and 15 MeV; the penetration depth of the first layer (X_1) is kept constant at the value of 1 mfp. At incident energies of 0.015 MeV, the contribution of the DLEBF and DLEABF values is higher for the AB combination than for BA, but at the higher energy of the incident gamma photon, i.e., at 15 MeV, the contribution of BA is higher than of AB. At a lower energy of 0.015 MeV, the photons interact first with PVA+50%Bi_2O_3 , which is a high-Z_{eff} layer, and consequently most of the photons undergo a photoelectric effect — thus very few photons undergo Compton scattering in the second layer. As thickness increases, the contribution of AB increases, but the BA contribution decreases. However, at a 15 MeV incident

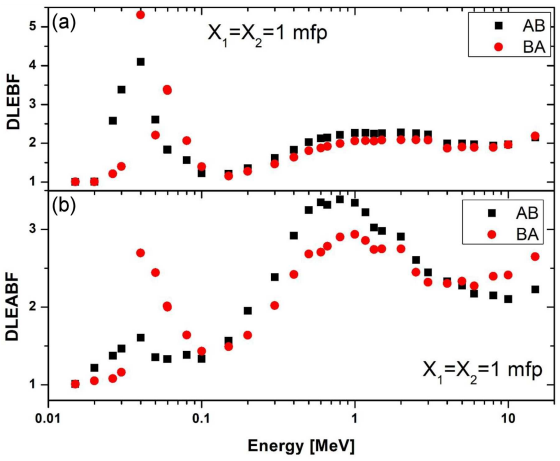

Fig. 3. (a)–(b) Factors DLEBF and DLEABF versus photon energy of double layers of high-Z-doped PVA polymers at selected penetration depth (X_1 = 1 mfp, and X_2 = 1 mfp). Here, X_1, and X_2 indicate the penetration depth of the first and second layer, respectively.

photon energy, not only the contribution of BA is higher than of AB, but also the contribution of BA is about 3 times higher than the AB contribution at X_2 mean free path of 40. This may be due to the fact that in the AB combination, the first layer is PVA+50%Bi_2O_3, which is a high-Z_{eff} layer, and the second layer is PVA+50%Na_2O_4W, which is a low-Z_{eff} layer comparatively to PVA+50%Bi_2O_3. In turn, in the BA combination, the first layer is PVA+50%Na_2O_4W, which is a low-Z_{eff} layer, and the second layer is PVA+50%Bi_2O_3, which is a high-Z_{eff} layer. Here, gamma photons interact first with B to produce Compton scattered gamma photons as it is a low-Z_{eff} material. These Compton scattered gamma photons are absorbed in high-Z_{eff} material A through the photoabsorption process. However, at 15 MeV of incident gamma photon, the pair production process is dominant and, consequently, the electron–positron pairs are produced in B, and these positrons annihilate with electrons to produce annihilation radiation of 1.02 MeV. These secondary gamma photons would contribute to the increase in the intensity of primary gamma photons as the penetration depth increases. Therefore, Figs. 4d and 5d show that the BA combination has higher values of DLEBF and DLEABF than the AB combination. It is a well-known fact that pair production depends on Z^2 [23]. So, high-Z_{eff} layers have higher values of DLEABF, and DLEBF lower than Z_{eff} layers.

For triple layers of high-Z-doped PVA polymers, there are six combinations, namely AAB, ABA, ABB, BAA, BAB, and BBA. The MLEBF (multilayer exposure buildup factor) and MLEABF (multilayer energy absorption buildup factor) values for triple layers of six combinations were calculated and presented in Figs. 6 and 7 as a function of

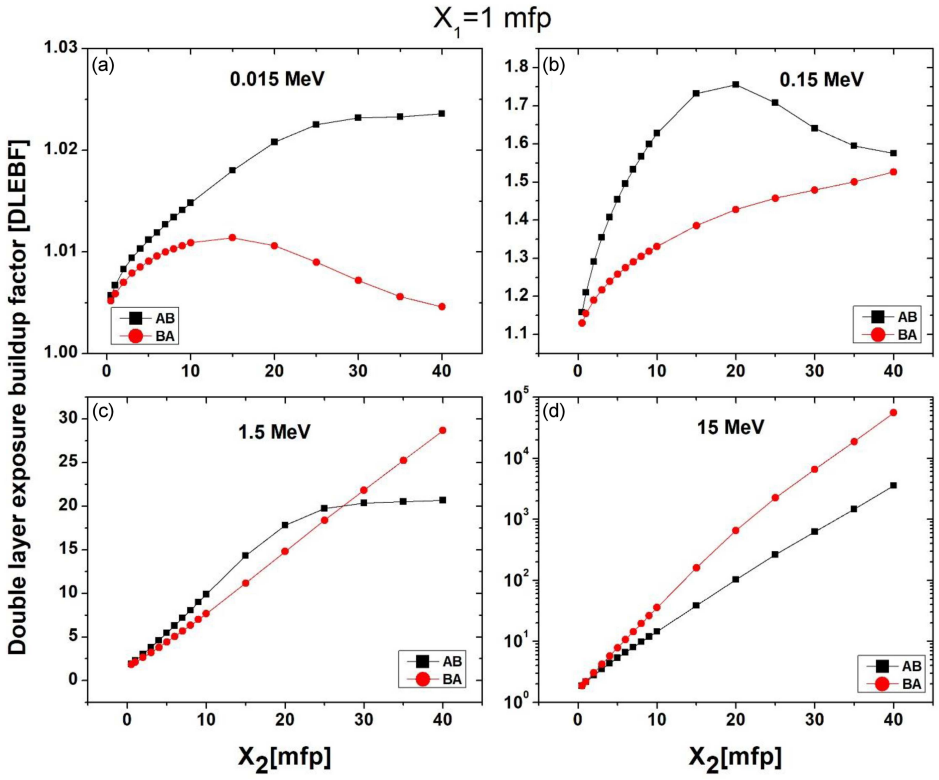

Fig. 4. (a)–(d) Factor DLEBF versus penetration depth of double layers of high-Z-doped PVA polymers at selected photon energy of 0.015, 0.15, 1.5, and 15 MeV. Here, X_1 and X_2 indicate penetration depth of the first and second layer, respectively.

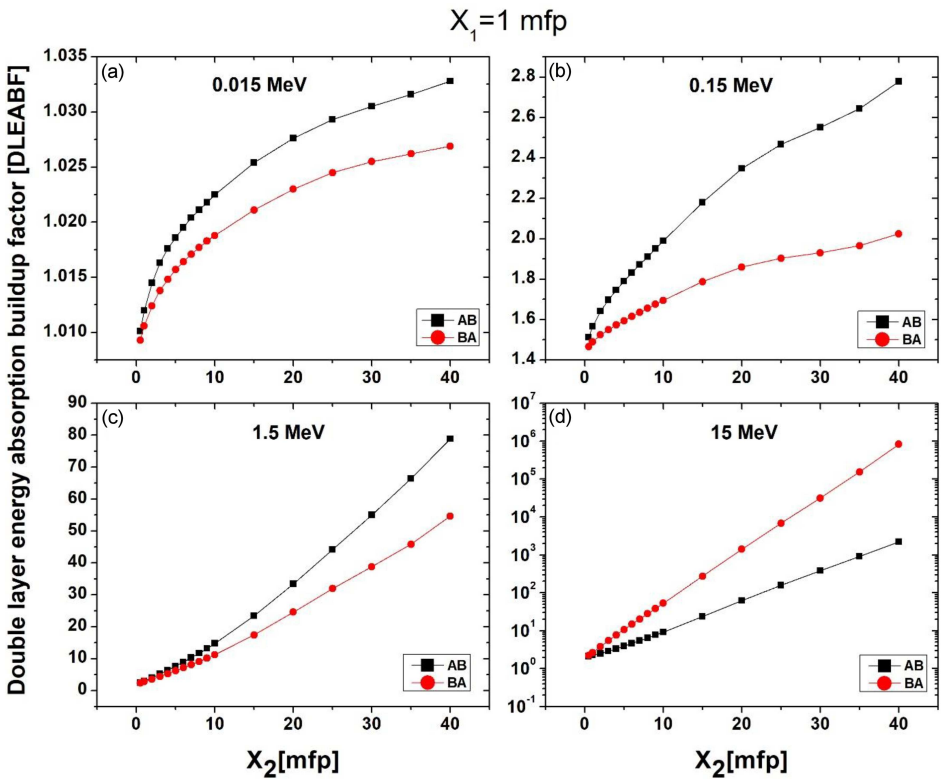

Fig. 5. (a)–(d) Factor DLEABF versus penetration depth of double layers of high-Z-doped PVA polymers at selected photon energy of 0.015, 0.15, 1.5, and 15 MeV. Here, X_1 and X_2 indicate penetration depth of the first and second layer, respectively.

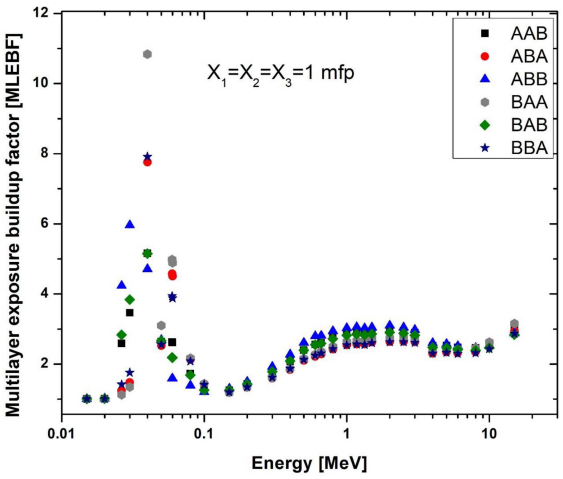

Fig. 6. Factor MLEBF versus photon energy of triple layers of high-Z-doped PVA polymers at selected penetration depth ($X_1 = 1$ mfp, $X_2 = 1$ mfp, and $X_3 = 1$ mfp). Here, X_1, X_2, and X_3 indicate the penetration depth of the first, second, and third layer, respectively.

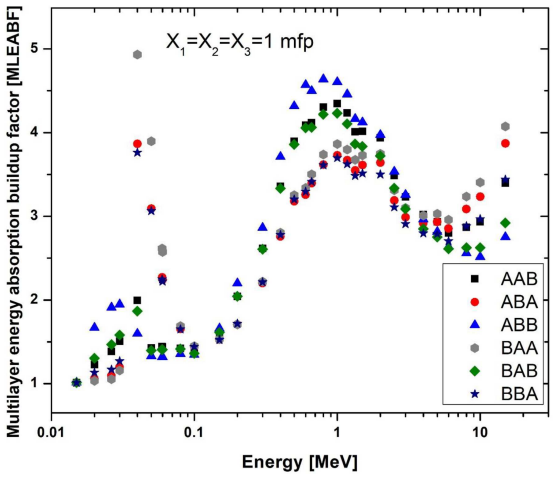

Fig. 7. Factor MLEABF versus photon energy of triple layers of high-Z-doped PVA polymers at selected penetration depth ($X_1 = 1$ mfp, $X_2 = 1$ mfp, and $X_3 = 1$ mfp). Here, X_1, X_2, and X_3 indicate the penetration depth of the first, second, and third layer, respectively.

the gamma photon energy at selected penetration depths. Here, X_1, X_2, and X_3 indicate the penetration depth [mfp] of the first, second, and third layers, respectively. Figures 6 and 7 show the MLEBF and MLEABF values for six triple combinations of high-Z-doped PVA polymers in the energy range from 0.01 to 15 MeV at penetration depths of $X_1 = 1$ mfp, $X_2 = 1$ mfp, and $X_3 = 1$ mfp. These figures show that among the six combinations of triple layers, both the MLEBF and MLEABF values peak around 1 MeV. At the peak position, the combination ABB has higher values and ABA has the lowest. It can be noticed from the combination ABB that the first layer is a high-Z material and the second and third layers are of low-Z. In the intermediate energy region, the Compton scattering process plays an important role in creating multiple scatterings. The multiple scattering increases in two low-Z materials. When 1.02 MeV gamma photons are incident on high-Z materials, they can undergo pair-production predominantly by creating electrons and positrons. These positrons annihilate electrons in the materials to produce two 511 keV gamma photons. These photons undergo Compton scattering in two low-Z materials. Because of the Compton scattering of 511 keV gamma photons, the buildup factor increases for ABB at 1 MeV. However, in the case of BBA, around 1 MeV, gamma photons first interact with low-Z material to produce the Compton scattered gamma photons. These scattered gamma photons again interact with low-Z materials to produce Compton scattered photons. In high-Z materials, these Compton scattered photons undergo photoelectric absorption to produce photoelectrons. These electrons are absorbed in the materials, and consequently, the buildup factor decreases. It has already been noticed from Fig. 3a–b that the combination BA has the lowest values of DLEBF and DLEABF. Similarly, the combinations ABA, BBA have the lowest values of MLEBF and MLEABF. Figures 8a–d and 9a–d show a plot of the MLEBF and MLEABF values as functions of penetration depth [mfp] at selected energies of 0.015, 0.15, 1.5, and 15 MeV. Here, $X_1 = 1$ mfp, $X_2 = 1$ mfp are kept constant, but X_3 is varied from 0 to 40 mfp, as shown in Figs. 8a–d and 9a–d. MLEBF and MLEABF as functions of penetration depth show similar behavior to DLEBF and DLEABF as functions of penetration depth. The combinations ABA and BBA have the lowest values of MLEBF and MLEABF at 0.015, 0.15, and 1.5 MeV.

Figure 10a–b shows buildup factors versus photon energy for a single and double layer of high-Z-doped PVA polymers at selected penetration depths. Here, for single layers (A and B): $X_1 = 2$ mfp, and for double layers (AB and BA): $X_1 = 1$ mfp and $X_2 = 1$ mfp. Figure 10 is to understand the potential of double-layered high-Z-doped PVA polymers compared to single-layered high-Z-doped PVA polymers. It is clear from Fig. 10a–b that double-layered combination BA has lower buildup factor values than a single-layered one. Further, it also indicates that double-layer combination BA is more suitable as radiation shields than a single-layered PVA+50%Bi_2O_3. Figure 11a–b shows the buildup factors versus photon energy of a single and triple layer of high-Z-doped PVA polymers at selected penetration depths. Here, for single layer (A and B): $X_1 = 3$ mfp, and for triple layer (ABA, BAA, and BBA): $X_1 = 1$ mfp, $X_2 = 1$ mfp, and $X_3 = 1$ mfp. Among six combinations, three (ABA, BAA, and BBA) are selected because these combinations

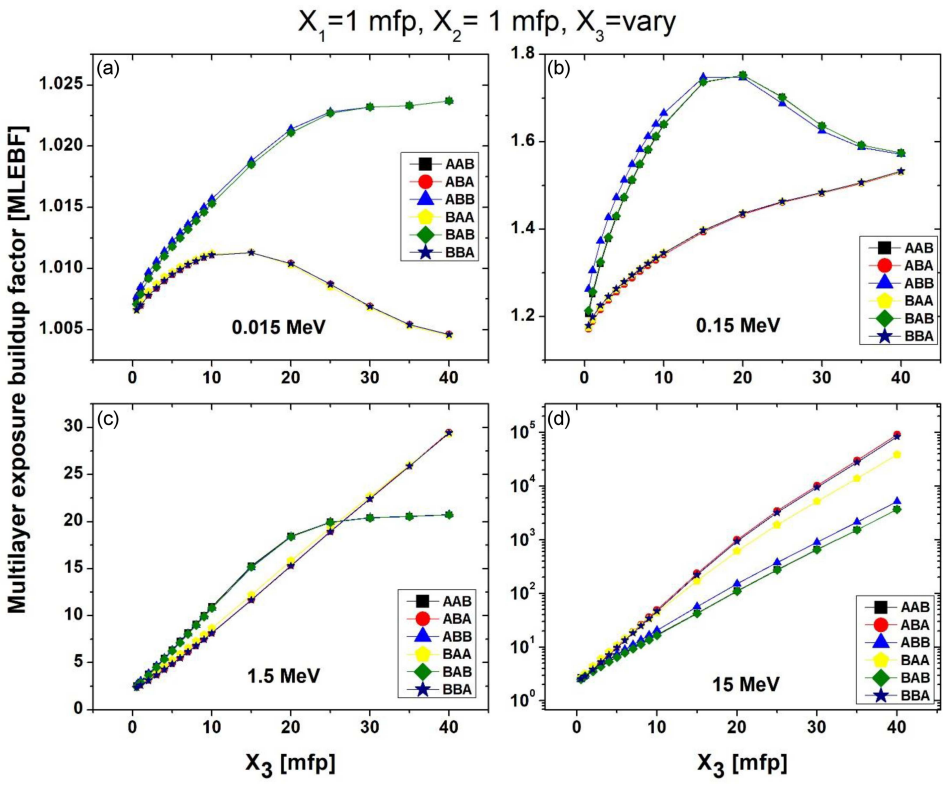

Fig. 8. (a)–(d) Factor MLEBF versus penetration depth of double layers of high-Z-doped PVA polymers at selected photon energy of 0.015, 0.15, 1.5, and 15 MeV. Here, X_1, X_2, and X_3 indicate the penetration depth of the first, second, and third layer, respectively.

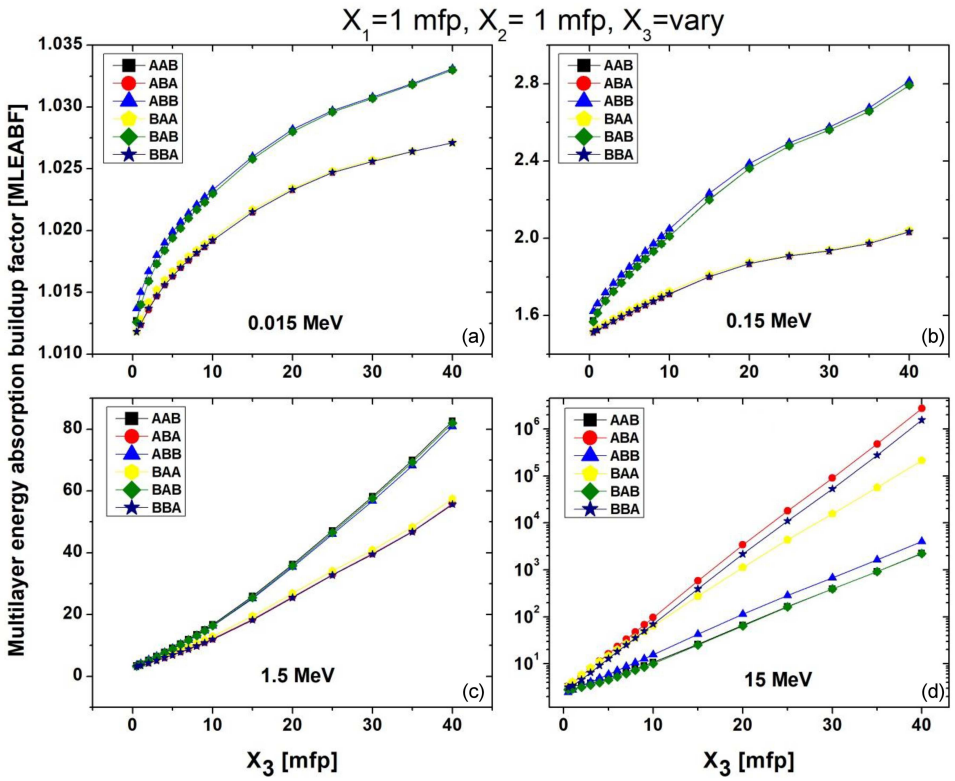

Fig. 9. (a)–(d) Factor MLEABF versus penetration depth of double layers of high-Z-doped PVA polymers at selected photon energy of 0.015, 0.15, 1.5, and 15 MeV. Here, X_1, X_2, and X_3 indicate the penetration depth of the first, second, and third layer, respectively.

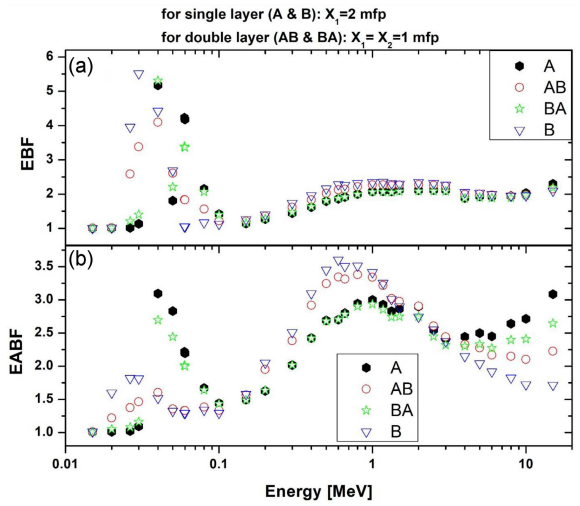

Fig. 10. (a)–(b) Buildup factors versus photon energy of single and double layers of high-Z-doped PVA polymers at selected penetration depth.

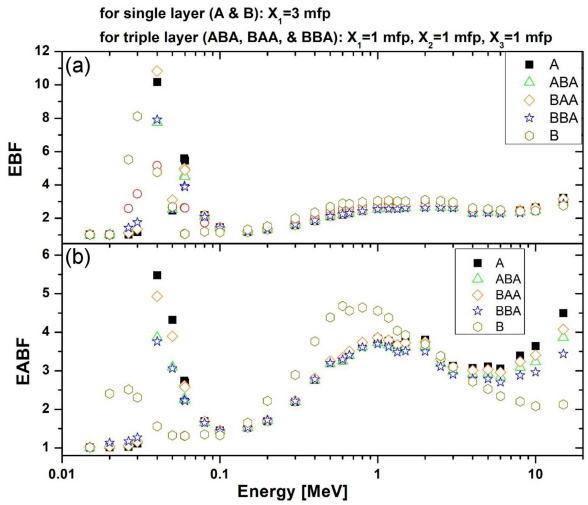

Fig. 11. Buildup factors versus photon energy of single and triple layers of high-Z-doped PVA polymers at selected penetration.

have lower buildup factors compared to the others. It is clear from Fig. 11a–b that the triple layer has slightly lower buildup factors than single layer of PVA+50%Bi_2O_3. It indicates that a triple layer of high-Z-doped PVA polymers has the potential to replace single layers of high-Z-doped PVA polymers.

4. Conclusions

The high-Z-doped PVA polymers such as PVA+50%Bi_2O_3 and PVA+50%Na_2O_4W were selected, and their buildup factors for double and triple layers were studied using the Py-MLBUF software. For single layer, the mass attenuation coefficient MAC, effective atomic number, and half- and tenth-layer values were estimated using the Py-MLBUF software. MAC values of a single layer of high-Z-doped PVA polymers were compared with the XCOM values in order to validate calculations. Among double layers, the combinations BA have higher DLEABF values than the combinations AB. In the higher energy region around 1 MeV, both the DLEBF and DLEABF values are higher for AB combinations than for BA. Calculated results also show that the values of DLEBF and DLEABF depend on the penetration depth of layers A and B. At a lower energy of 0.015 MeV, the DLEBF and DLEABF values are higher for AB combinations than for BA. However, at higher energy at 15 MeV, BA has higher DLEBF and DLEABF values than AB. This indicates that the combination BA is more suitable as a radiation shield than AB. Moreover, it is interesting to notice that combinations may influence buildup factors. Among the triple layers, six combinations exist, and among these six, the combinations ABA and BBA have lower MLEABF and MLEBF values compared to other combinations. The BA and BBA combinations have the potential to replace the single layer of high-Z-doped PVA polymers, and these combinations can be used as gamma-ray shields. Therefore, the double- and triple-layered radiation shields not only overcome the void paths but can potentially replace the single-layered radiation shields. The double and triple layers play an important role in enhancing radiation shielding effectiveness.

References

[1] C.V. More, Z. Alsayed, Mohamed. S. Badawi, A.A. Thabet, P.P. Pawar, *Environ. Chem. Lett.* **19**, 2057 (2021).

[2] M.R. Ambika, N. Nagaiah, S.K. Suman, *J. Appl. Polym. Sci.* **134**, 44657 (2017).

[3] S.A. Tijani, Y. Al-Hadeethi, *Mater. Res. Express* **6**, 55323 (2019).

[4] J.M. Sharaf, H. Saleh, *Radiat. Phys. Chem.* **110**, 87 (2015).

[5] A. Thumwong, J. Darachai, K. Saenboonruang, *Polymers* **14**, (2022).

[6] D. Toyen, E. Wimolmala, K. Saenboonruang, *Polymers* **15**, 2717 (2023).

[7] K.S. Mann, *Radiat. Phys. Chem.* **159**, 207 (2019).

[8] K.S. Mann, M.S. Heer, A. Rani, *Radiat. Phys. Chem.* **125**, 27 (2016).

[9] M.V. Muthamma, S.G. Bubbly, S.B. Gudennavar, K.C.S. Narendranath, *J. Appl. Polym. Sci.* **136**, 47949 (2019).

[10] A.A. Abbas, B.A. Abdullah, M.A. abd Al-Hussain, *Basrah J. Sci.* **35**, 73 (2017).

[11] K.S. Mann, S.S. Mann, *Ann. Nucl. Energy* **150**, 107845 (2021).

[12] G.B. Hiremath, V.P. Singh, N.H. Ayachit, N.M. Badiger, *Radiol. Phys. Technol.* **16**, 168 (2023).

[13] G.B. Hiremath, M.M. Hosamani, V.P. Singh, N.H. Ayachit, N.M. Badiger, *J. Nucl. Eng. Radiat. Sci.* **9**, 032004 (2023).

[14] M.M. Hosamani, A. Vinayak, G.B. Hiremath, P.N. Patil, N.M. Badiger, *Ann. Nucl. Energy* **171**, 109045 (2022).

[15] S.B. Kolavekar, G.B. Hiremath, N.M. Badiger, N.H. Ayachit, *Nucl. Sci. Eng.* **197**, 1506 (2023).

[16] S.B. Kolavekar, G.B. Hiremath, P.N. Patil, N.M. Badiger, N.H. Ayachit, *Heliyon* **8**, e11788 (2022).

[17] G.B. Hiremath, N.H. Ayachit, N.M. Badiger, *Radiat. Effects Defects Solids* **178**, 1038 (2023).

[18] K. Hanamar, G.B. Hiremath, B.G. Hegde, N.H. Ayachit, N.M. Badiger, *Optik* **273**, 170397 (2023).

[19] G.B. Hiremath, M.M. Hosamani, A. Vinayak, P.N. Patil, V.P. Singh, N.H. Ayachit, N.M. Badiger, *Radiat. Effects Defects Solids* **178**, 3335 (2023).

[20] M.M. Hosamani, A. Vinayak, S. Mangeshkar, S. Malode, S. Bhajantri, V. Hegde, G.B. Hiremath, N.M. Badiger, *Spectrosc. Lett.* **53**, 132 (2020).

[21] G.B. Hiremath, M.M. Hosamani, A. Vinayak, P.N. Patil, V.P. Singh, N.H. Ayachit, N.M. Badiger, *Radiat. Effects Defects in Solids* **178**, 335 (2023).

[22] U.T. Lin, S.H. Jiang, *Radiat. Phys. Chem.* **48**, 389 (1996).

[23] N.A. Dyson, in: *X-Rays in Atomic and Nuclear Physics*, 2nd ed., Cambridge University Press, Cambridge 1990, p. 198.

[24] M. Berger, J. Hubbell, "XCOM: Photon cross sections on a personal computer", National Bureau of Standards, Center for Radiation Research, Washington DC 1987.